15

STOCHASTIC MODELS OF SINGLE CELLS

The majority of experiments in neurophysiology are based upon *spike trains* recorded from individual or multiple nerve cells. If all the action potentials are taken to be identical and only the times at which they are generated are considered, the experimentalist obtains a discrete series of time events $\{t_1, \cdots, t_n\}$, where t_i corresponds to the occurrence of the ith spike, characterizing the spike train. This spike train is transmitted down the axon to all of the target cells of the neuron, and it is this spike train that contains all of the relevant information that the cell is representing (assuming no dendro-dendritic connections).[1]

As alluded to in the preceding chapter, there are two opposing views of neuronal coding, with many interim shades. One view holds that it is the firing *rate*, averaged over a suitable temporal window (Eqs. 14.1 or 14.2), that is relevant for information processing. The dissenting view, *correlation coding*, argues that the interactions among spikes, at the single cell as well as between multiple cells, encodes information.

A key property of spike trains is their seemingly *stochastic* or random nature, quite in contrast to switching in digital computers.[2] This randomness is apparent in the highly irregular discharge pattern of a central neuron to a sensory stimulus whose details are rarely reproducible from one trial to the next (Figs. 14.1 and 15.1). The apparent lack of reproducible spike patterns (but see Fig. 15.11) has been one of the principal arguments in favor of the hypothesis that neurons only care about the firing frequency averaged over very long time windows. Such a *mean rate code* is very robust to "sloppy" hardware but is also relatively inefficient in terms of transmitting the maximal amount of information per spike. Encoding information in the intervals between spikes is obviously much more efficient, in particular if correlated across multiple neurons. Such a scheme does place a premium on postsynaptic neurons that can somehow decode this information.

Because little or no information can be encoded into a stream of regularly spaced action potentials, this raises the question of how variable neuronal firing really is. How

1. Slower processes, such as extracellular potassium accumulation or local depletion of calcium, could also play a role in information transmission among cells. Since very little is known about these, we neglect them for now; see, however, the penultimate chapter.

2. We use the term "seemingly" on purpose. It may well be that what we think of as noise is the signal we are seeking!

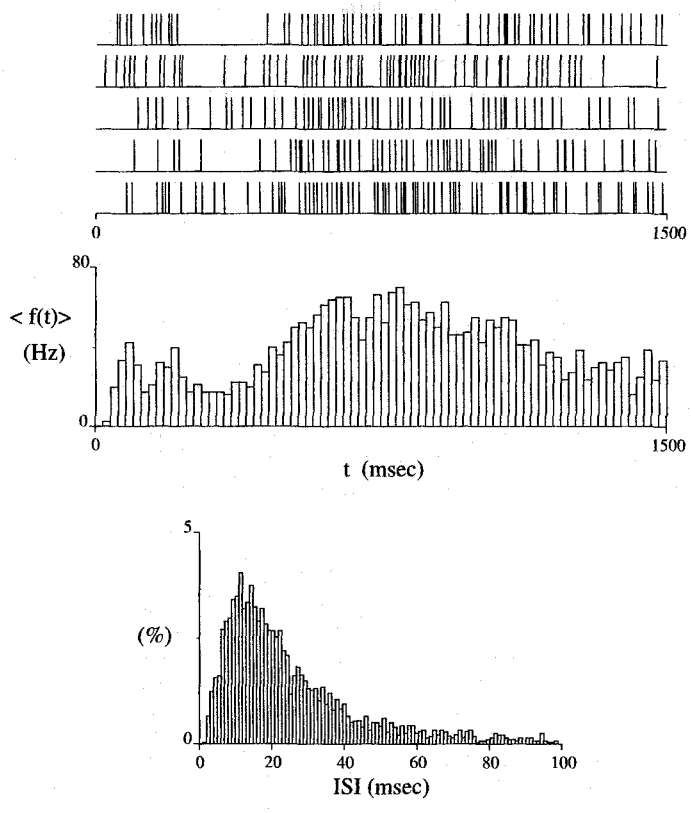

Fig. 15.1 **Variability of Neuronal Spiking** A high-contrast bar is swept repeatedly over the receptive field of a cortical cell in the awake macaque monkey. Much variability in the microstructure of spiking is evident from trial to trial. The poststimulus time histogram in the middle corresponds to the averaged firing rate $\langle f(t) \rangle$ (using 20 msec bins) taken over 40 trials. The lower plot illustrates the associated interspike interval (ISI) histogram. It shows a lack of very short intervals, indicative of a refractory period, and an exponentially decreasing likelihood of finding very large gaps between spikes. The lack of reproducibility of the detailed spike pattern is the primary reason arguing for the idea of a mean rate code (Eq. 14.1). Yet neurons deep within the cortex can faithfully reproduce the microstructure of spiking over several hours (Fig. 15.11). From W. Newsome, K. Britten, personal communication.

can the observed randomness be explained on the basis of the cell's biophysics and synaptic input (Calvin and Stevens, 1968; Softky and Koch, 1993; Shadlen and Newsome, 1994; Softky, 1995; König, Engel, and Singer, 1996)? The mathematical theory of stochastic point processes and the field of statistical signal processing offer a number of tools adequate for analyzing the properties of spike trains. We will study these here and will relate them to simple models of biophysics. This will enable us to infer something about the integrative mechanisms underlying neuronal firing activity.

In the previous chapter we exclusively dealt with deterministic input $I(t)$ to spiking neurons. Given the highly stochastic nature of neurons evident in Fig. 15.1, it is imperative that we now begin to deal with *random variables*, that is, observables that take on discrete (such as the number of spikes) or continuous (such as the membrane potential) values with certain probabilities. For an introduction into the field, we refer the reader to Papoulis (1984); for monographs on stochastic neural activity, see Holden (1976), Tuckwell (1988c), and Smith

(1992). Gabbiani and Koch (1998) should be read as a complementary text to this chapter, as they discuss in more detail signal processing approaches toward spike train analysis and their numerical implementation into a suite of freely available MATLAB routines.

15.1 Random Processes and Neural Activity

For starters, let us assume that we are dealing with discrete random variables. We consider a *stochastic* or *random process*, that is, a family of such random variables parameterized by time t. In other words, at every instant t the random process has the discrete value $N(t)$, while the entire process is specified by $\{N(t), t \geq 0\}$. In the following, we are frequently faced by questions of the form: "What is the probability that N is as large as some specific n_{th}?" In order to answer these, we need to specify a probability distribution from which the random variable N is drawn. Before we do so, let us remind our readers of several important concepts.

One is the idea of a *point process*, which is simply a process that can be mapped onto a set of random points on the time axis. Two examples of point processes are the occurrence of action potentials and the times at which a synaptic vesicle is relased at some synapse. A point process is described by a series of delta pulses, $\sum \delta(t - t_i)$.

We can introduce a new random variable, defined as the interval between consecutive events, $T_i = t_{i+1} - t_i$, to help us introduce the notion of a *renewal process*. This is a point process in which the random variables T_i are independent and identically distributed. The notion of a renewal process comes from industrial practice: the probability that some machine will fail within some interval is identical for all machines and will not vary from one interval to the next. Applied to a spike train, it would imply that the chance of finding some particular interspike interval (Fig. 15.1) is independent of whether a short or a long interspike interval preceded it. This does tend to be true to a first approximation for many cortical cells. On the other hand, it is certainly not true for bursting cells, where the probability for finding a long interspike interval after two or three very short ones is strongly enhanced (see the following chapter). Renewal processes are much simpler to describe from a mathematical point of view than nonrenewal processes. Lastly, a *stationary* stochastic process (or a random process) is one whose statistical properties do not depend on the time of observation but remain constant in time.

Since true stationarity is very difficult to verify in practice, it is common to use the less stringent concept of a *wide-sense* or *weakly stationary* process. This is a random process whose mean is constant and whose autocorrelation function only depends on $t - t'$, that is, a process whose first- and second-order statistical properties are time invariant.

Let us now focus on the most common discrete renewal process, the *Poisson process*.

15.1.1 Poisson Process

A Poisson process is the simplest possible random process with no memory and is characterized by a single parameter, the *rate* or *mean frequency* μ. It is of great relevance to neurobiology, since a number of discrete biophysical events appear to follow a Poisson distribution closely. The best studied example of a Poisson process is the spontaneous release of individual packets of the neurotransmitter acetylcholine at the frog neuromuscular junction (Fatt and Katz, 1952; for an overview see Stevens, 1993, and Chap. 4.2). At the postsynaptic terminal this release gives rise to so-called *miniature endplate potentials*,

whose arrival times can be accurately modeled by a Poisson process. As we will see below, the distribution of action potentials in cortical cells can be approximated to a certain degree by a modified Poisson process.

A number of different, but equivalent, definitions of a Poisson process exists. We define $\{N(t), t \geq 0\}$ to be a simple *Poisson process* with mean rate μ if:

1. Given any $t_0 < t_1 < t_2 < \cdots < t_{n-1} < t_n$, the random variables $N(t_k) - N(t_{k-1})$, $k = 1, 2, \cdots, n$, are mutually independent.
2. For any $0 \leq t_1 < t_2$ the average number of events occurring between t_1 and t_2 is $\mu(t_2 - t_1)$.

The first condition specifies that the number of events occurring in one interval is independent of the number of events occurring in any other interval, provided they do not overlap. The second property tells us that the expected number of events is proportional to the rate times the duration of the interval.

As no point in time is singled out in this definition of the Poisson process, it is a *stationary* process.

It follows from these conditions (Feller, 1966) that the actual number of events, $N(t_2) - N(t_1)$, is a random variable with the Poisson probability distribution

$$\Pr\{N(t_2) - N(t_1) = k\} = \frac{(\mu(t_2 - t_1))^k e^{-\mu(t_2 - t_1)}}{k!} \tag{15.1}$$

with $k = 0, 1, 2, \cdots$.

The parameter μ specifies the average number of events per unit time. With $t_1 = t$ and $t_2 = t + \Delta t$, we have for the probability that exactly k events occur in the interval Δt,

$$\Pr\{N(t + \Delta t) - N(t) = k\} = \frac{(\mu \Delta t)^k e^{-\mu \Delta t}}{k!}. \tag{15.2}$$

If $\mu \Delta t \ll 1$, that is, if much less than one event is expected to occur in the interval Δt, the e^{-x} term in Eq. 15.2 can be expanded into a Taylor series $1 - x + x^2/2 - x^3/3 + \cdots$. We then have for the probability that none or a single event occurs in the interval Δt,

$$\Pr\{N(t + \Delta t) - N(t) = 0\} = e^{-\mu \Delta t} \approx 1 - \mu \Delta t \tag{15.3}$$

$$\Pr\{N(t + \Delta t) - N(t) = 1\} = \mu \Delta t e^{-\mu \Delta t} \approx \mu \Delta t\,. \tag{15.4}$$

These estimations are accurate within $(\Delta t)^2$, that is, the error in these estimates goes as a polynomial of order $(\Delta t)^2$ to zero as $\Delta t \to 0$. In other words, as the product of the average firing frequency and the interval is made smaller and smaller the approximation becomes better and better. Figure 15.2 illustrates how the events generated by a Poisson process are distributed compared to the spike distribution taken from a neuron. Both processes have the same overall rate. On account of the refractory period, we modified the Poisson process to prevent two spikes from directly following each other.

A commonly used procedure for numerically generating Poisson distributed action potentials with mean rate μ is based on this approximation. A random number r, uniformly distributed between 0 and 1, is generated for every interval Δt; if $r \leq \mu \Delta t$, a spike is presumed to have occurred between t and $t + \Delta t$; otherwise, no spike is generated. (This assumes that the probability of generating a spike in the interval considered, that is, $\mu \Delta t$ is much less than one.)

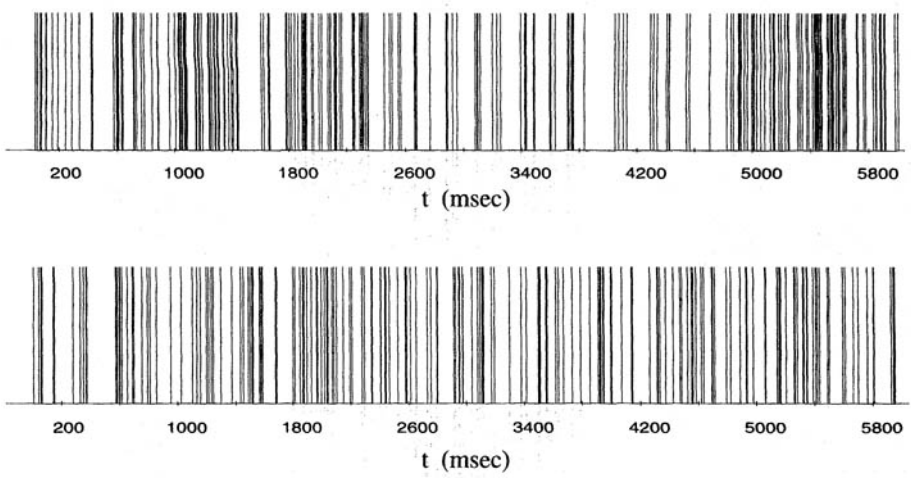

Fig. 15.2 SPIKE TRAINS AND THE RANDOM POISSON PROCESS Spike train from an extracellularly recorded cell in the parietal cortex of a behaving monkey (upper trace; data kindly provided by J. Fuster) and from a synthetic Poisson process with a refractory period of 1 msec (lower trace). The mean firing rate of both processes is 30 Hz. Notice the relatively rare occurrences of large gaps between spikes. In a Poisson process, the probability of occurrence of gaps of duration T decreases as $e^{-T\mu}$.

15.1.2 Power Spectrum Analysis of Point Processes

A number of signal processing techniques rely on evaluating average spike train properties in response to random stimulus ensembles. This works best if the system at hand can be described as a linear, time-invariant one. Under these conditions, the *power spectrum* $S(f)$ of the associated spike train reveals details about the filter function that is used by the system (e.g., does the neuron act as a low-pass or as a band-pass filter?).

A basic result of the theory of stochastic processes (Papoulis, 1984) is that the power spectrum of a Poisson process is flat at all frequencies except for a delta peak at the origin. To be more precise, the spectrum associated with an infinite train of delta impulses distributed according to a Poisson process of rate μ is

$$S(f) = \mu + 2\pi\mu^2\delta(f)\,. \tag{15.5}$$

This is in accordance with our intuition that all spectral components should be equally represented in a completely random spike train; no particular frequency (such as $1/\mu$) is singled out. The *autocorrelation function*, defined as the inverse Fourier transform of the power spectrum, has a similar shape, taking on a constant value of μ^2 everywhere except at the origin, where it is a $\delta(t)$ function.

Neurons, however, do not fire totally without memory, due to the presence of a refractory period. A mathematically convenient manner in which this can be accounted for (Perkel, Gerstein, and Moore, 1967; Bair et al., 1994) is by introducing the *renewal density function*, which denotes the probability for a spike to occur between $t_1 + t$ and $t_1 + t + dt$, given that a spike was just generated at t_1. For a pure Poisson process, the renewal density function is a constant equal to the rate. In our case, however, the renewal density has a dip around zero, indicating a reduced probability of spiking due to the refractory period. This can easily be measured experimentally. Assuming that the dip due to the refractory period can be accounted for by a Gaussian of variance σ_{ref}^2, the associated power spectrum is,

$$S(f) = \mu(1 - \sqrt{2\pi}\mu\sigma_{\text{ref}}e^{-2(\pi f\sigma_{\text{ref}})^2}) + 2\pi\mu^2\delta(f)\,. \tag{15.6}$$

To ensure that the power is always positive, the maximum firing rate must be limited: $\mu \leq 1/(\sqrt{2\pi}\sigma_{\text{ref}})$. This spectrum, parameterized by the mean rate μ and the width of the refractory period σ_{ref} is constant for large values of f but dips toward its minimum at $f = 0$ (Fig. 15.3). A longer refractory period (that is, a larger value of σ_{ref}) causes a deeper trough at low frequencies. Note that this result appears at odds with intuition, since a refractory period seems to demand a dip in the neighborhood of the inverse of the smallest interspike interval, that is, at high temporal frequencies.

A mathematically more general manner to account for the refractory period is by postulating that the interspike intervals are independently and identically distributed random variables, which themselves are the sum of a random refractory period and a statistically independent interval due to a known stationary process (Franklin and Bair, 1995).

Spike train analysis of cortical cells (Bair et al., 1994) showed that the spectrum of 40% of these neurons can be fitted using Eq. 15.6 (left column in Fig. 15.3). The good match between the analytical model, experimental data, and synthetic spike train supports the hypothesis that once the refractory period is accounted for, a Poisson hypothesis constitutes a first-order description of cortical spike trains.

15.2 Stochastic Activity in Integrate-and-Fire Models

Let us now take an integrate-and-fire model, as described in the previous chapter, and bombard it with stochastic, Poisson distributed, synaptic inputs. In what is to come, we will neglect the membrane leak, as well as adaptation and the refractory period, to get at the principle underlying stochastic activity in these models. Using the nonleaky

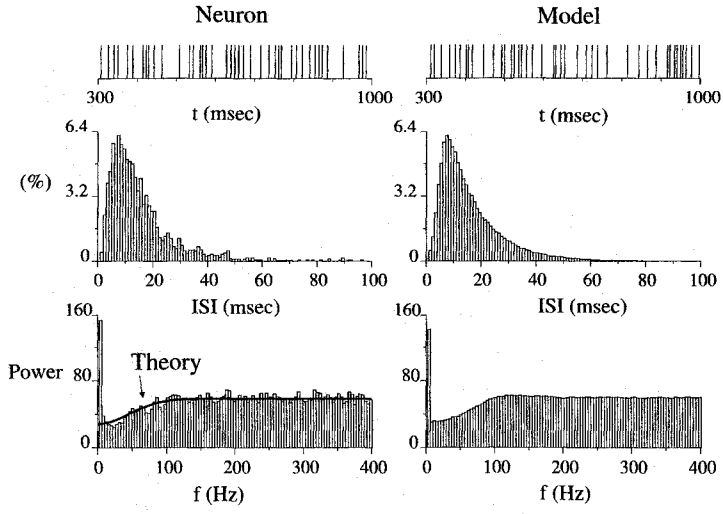

Fig. 15.3 Power Spectrum of Cortical Cells Representative spike train, interspike interval histogram, and power spectrum for a neuron recorded from cortical area MT in a behaving monkey (left column) compared against a modeled point process (right column). The synthetic data assume that spikes are Poisson distributed with an absolute refractory period drawn from a Gaussian distribution (of 5 msec mean and 2 msec standard deviation). Equation 15.6 has been fitted to the neuron's spectrum (curve labeled "Theory") with $\mu = 58$ Hz, and $\sigma_{\text{ref}} = 3.5$ msec). The spectrum of many nonbursting cells can be fitted against this simple model, which satisfactorily captures many aspects of their random behavior. Reprinted in modified form by permission from Bair et al., (1994).

integrate-and-fire model allows us to derive closed-form expressions for many variables of interest. Conceptually, $R = 0$ corresponds to a cell for which the time between spikes is much shorter than the membrane time constant, so that the decay of the membrane potential can be neglected. We later investigate $R \neq 0$ using numerical simulations.

We assume that the integrator cell receives excitatory synaptic input from a Poisson distributed random process $N_e(t)$ with mean rate μ_e and synaptic weight a_e. Conceptually, each synaptic input can be thought of as dumping a_e amount of charge onto the capacitance C, raising the membrane potential by a_e/C toward threshold. We assume here that C has been folded into the synaptic weight a_e; it will not be included in the equations to come (equivalently, $C = 1$). The random process $V(t)$, that is, the membrane potential, shows random jumps of amplitude a_e. In the absence of a threshold, the membrane potential can be described as

$$V(t) = a_e N_e(t) . \tag{15.7}$$

15.2.1 Interspike Interval Histogram

Let us proceed methodically by first starting with trivial cases, working up to more complex situations. In this spirit, we assume that $a_e \geq V_{\text{th}}$, that is, each synaptic input is, by itself, sufficient to cause a spike. (Think of a single retinal ganglion cell making a few hundred synaptic contacts on a single geniculate relay cell.) Trivially, the probability distribution of the output spike will be identical to that of the synaptic input.

If the perfect integrator generated a pulse at $t = 0$ and was reset, what is the waiting time T_1 for the next output pulse to occur? In the case of $a_e \geq V_{\text{th}}$, this is equivalent to asking what is the waiting time for the next synaptic input to occur. This function can be computed if we know the probability for no event to occur between $(0, t)$, which is

$$\Pr\{T_1 > t\} = \Pr\{N(t) - N(0) = 0\} = e^{-\mu_e t} . \tag{15.8}$$

The distribution function for the next spike to occur is one minus this result, that is, $1 - e^{-\mu_e T}$; the longer one waits, the more likely an input is to occur. The probability density function $p_1(t)$ for t is the temporal derivative of the distribution function,

$$p_1(t) = \mu_e e^{-\mu_e t} . \tag{15.9}$$

The choice of our initial observation point, here $t = 0$, does not affect this result since the Poisson process is ahistoric. This is an important point to note; the density function does not depend on whether or not an event just occurred. (Of course, given the existence of a refractory period, this will not be true for real neurons at very small time scales.) Therefore, $p_1(t)$ corresponds to the density of time intervals between adjacent pulses.

The average duration between events is

$$\langle t \rangle = \int_0^\infty t p_1(t) dt = \frac{1}{\mu_e} \tag{15.10}$$

justifying our interpretation of μ_e as the mean rate.

What happens if we assume that n_{th} inputs are needed to trigger a pulse (with $n_{\text{th}} = \lfloor V_{\text{th}}/a_e + 1 \rfloor$, where $\lfloor x \rfloor$ is the largest integer less than or equal to x)? This is similar to a Geiger counter that is rigged to click every time it detects n_{th} radioactive decays. Answering this question requires us to compute the time T_{th} in which we expect a Poisson process with rate μ_e to generate exactly n_{th} events. This is given by the probability for $n_{\text{th}} - 1$ events to occur between now and t, multiplied by the probability for a single event to occur in the interval $[t, t + \delta t)$,

$$\Pr\{T_{\text{th}} > t + \delta t\} = \frac{(\mu_e t)^{n_{\text{th}}-1} \cdot e^{-\mu_e t}}{(n_{\text{th}} - 1)!}(\mu_e \delta t)\,. \tag{15.11}$$

The probability density function of T_{th} is the limit of this expression divided by δt as $\delta t \to 0$,

$$p_{n_{\text{th}}}(t) = \frac{\mu_e \cdot (\mu_e t)^{n_{\text{th}}-1} \cdot e^{-\mu_e t}}{(n_{\text{th}} - 1)!}\,. \tag{15.12}$$

This expression for the waiting time is known as the n_{th}th-order *gamma density*.

The density function $p_{n_{\text{th}}}(t)$ is obtained experimentally by binning consecutive interspike intervals from spike trains, as in Figs. 15.1 and 15.4. In this guise it is called the *interspike interval* (ISI) histogram. The mean interspike interval is

$$\langle T_{\text{th}} \rangle = \frac{n_{\text{th}}}{\mu_e} \tag{15.13}$$

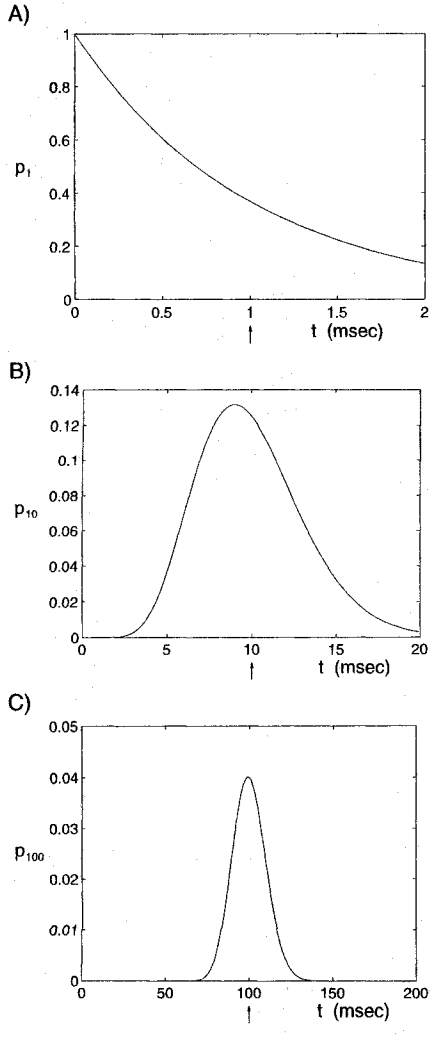

Fig. 15.4 Interspike Interval Distribution In the interspike interval distribution the occurrences of the intervals between adjacent spikes is histogrammed. This is done here analytically for pulses generated by a perfect integrate-and-fire unit that receives Poisson distributed input with a constant rate of $\mu = 1000$ (per second). The threshold of the unit varies, with **(A)** $n_{\text{th}} = 1$ (each input generates an output pulse), **(B)** $n_{\text{th}} = 10$, and **(C)** $n_{\text{th}} = 100$. The ISIs are gamma distributed (Eq. 15.12). As expected, the mean output rate decreases as the number of synaptic inputs needed to reach threshold n_{th} increases (the mean interspike interval is at 1, 10, and 100 msec for the three panels; see arrows). The normalized standard deviation, called the *coefficient of variation* C_V (Eq. 15.15) scales as $1/\sqrt{n_{\text{th}}}$. In other words, the relative jitter in the timing of output pulses becomes smaller as n_{th} becomes larger. If the cell is integrating over a significant number of small inputs, the ISI distribution approaches the normal distribution (as in **C**).

and the variance is

$$\mathrm{Var}[T_{\mathrm{th}}] = \frac{n_{\mathrm{th}}}{{\mu_e}^2}. \tag{15.14}$$

Figure 15.4 shows waiting time densities for a nonleaky integrate-and-fire neuron receiving excitatory input at a constant rate μ_e in which the effective voltage threshold is increased by a decade, corresponding to $n_{\mathrm{th}} = 1$, 10, and 100. As n_{th} of the gamma distribution increases, the probability density of the interspike intervals rapidly tends toward a Gaussian distribution.

15.2.2 Coefficient of Variation

The most common way to quantify interspike variability is via the normalized standard deviation, that is, the square root of the variance of the ISI histogram divided by its mean,

$$C_V = \frac{(\mathrm{Var}[T_{\mathrm{th}}])^{1/2}}{\langle T_{\mathrm{th}} \rangle}. \tag{15.15}$$

This measure is known as the *coefficient of variation*. For the perfect integrator model considered here, we have

$$C_V = \frac{1}{{n_{\mathrm{th}}}^{1/2}}. \tag{15.16}$$

For $n_{\mathrm{th}} = 1$, associated with an exponential ISI (Fig. 15.4A), $C_V = 1$. As the number of random inputs over which the unit integrates (or averages) becomes larger, the normalized ISI becomes narrower and narrower and C_V smaller and smaller (Fig. 15.4C). The relationship between spike train variability and C_V is illustrated graphically in Fig. 15.5.

This result can be explained qualitatively by invoking the *central limit theorem*, which states that as the number n of independent random variables x_i goes to infinity, the random variable defined by the mean of all x_i's, $\langle x \rangle = (1/n) \sum_{i=1}^{n} x_i$, has an asymptotically Gaussian distribution, with a mean identical to the mean of the population and with a standard deviation scaling as $1/\sqrt{n}$ of the standard deviation of the individual x_i's. If we were to compute the average height of all students in one class, there would be a great deal of variability around the mean. Yet the C_V associated with the average height of all men in the United States is minute. In other words, if a neuron can only be brought to fire action potentials by summing over dozens or more of independent synaptic inputs, it should fire very regularly. And as we noted above, a neuron with little variability in its interspike interval cannot readily exploit temporal coding (since little information can be encoded in a regular interspike interval).

Incorporating an absolute refractory period t_{ref} into the integrator shifts the interspike interval probability distribution by the same amount to the right. It gives the perfect integrator cell a characteristic time scale, so we cannot expect it to have identical statistics at all firing rates. The new C_V is

$$C_V = \frac{1}{{n_{\mathrm{th}}}^{1/2}} \frac{\langle T_{\mathrm{th}} \rangle - t_{\mathrm{ref}}}{\langle T_{\mathrm{th}} \rangle}. \tag{15.17}$$

The effect of the refractory period is to regularize the spike train, lowering its variability. This is particularly true for high firing rates, as $\langle T_{\mathrm{th}} \rangle$ approaches t_{ref}.

If we were to measure the interspike interval variability generated by a sustained current injection into an integrate-and-fire cell (Fig. 15.5E) or into a squid giant axon

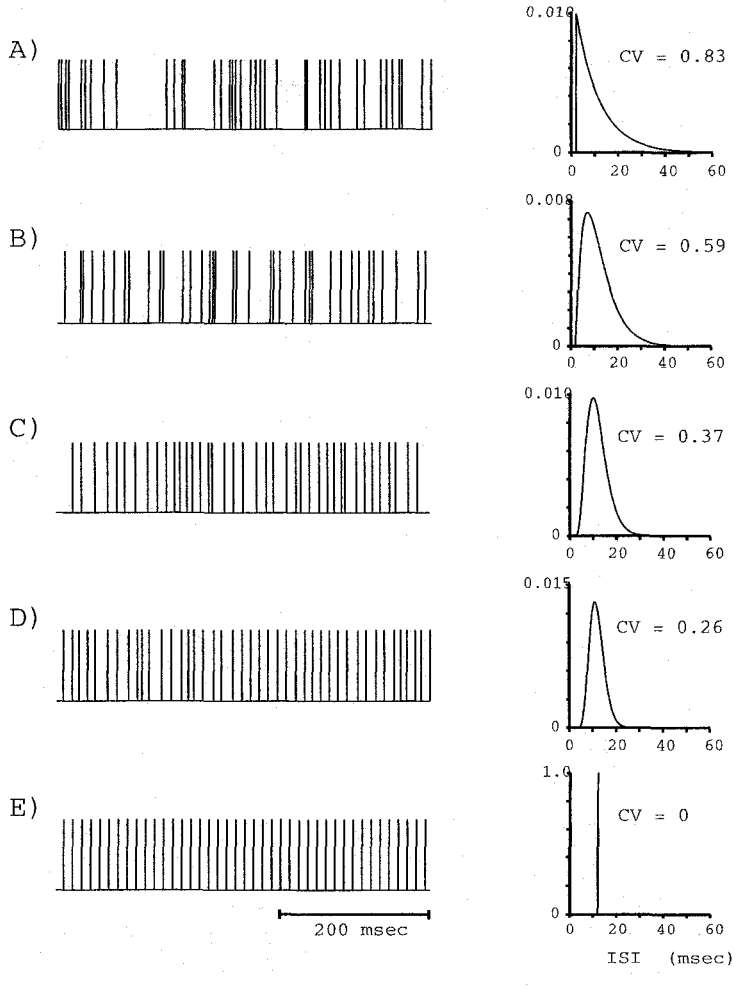

Fig. 15.5 Spike Train Interspike Variability Sample spike trains and interspike interval histograms for a perfect integrator model with an absolute refractory period t_{ref} of 2 msec for Poisson distributed synaptic input. The mean interspike interval is in all cases identical to 12 msec. **(A)** Each synaptic input gives rise to a spike. The ISI is a shifted exponential; the deviation of the associated C_V from unity reflects the regularizing effect of the refractory period. **(B)–(D)** n_{th} is increased to 2, 5, and 10, respectively. To retain the same average firing frequency, the input firing frequency was also increased by the same amount. The ISI can be described by a gamma density (Eq. 15.12). **(E)** Response to a sustained current injection.

(see Fig. 6.9), it would tend to zero. Biological pacemaking systems like the heart or the rhythm underlying breathing have C_V's in the low percent range. In some systems the C_V can be a miniscule fraction of one percent. The neurons in the weakly electric fish *Eigenmannia* that are responsible for triggering the clocklike electric organ discharge in the 0.1–1 kilohertz frequency range have a spike jitter of less than 1 μsec (Kawasaki, Rose, and Heiligenberg, 1988).

In all of these examples, $C_V \leq 1$, with the upper bound given by a pure Poisson process. Yet in many instances interspike interval distributions of real neurons have C_V's greater than 1 (Wilbur and Rinzel, 1983; see also Sec. 16.1). This can be achieved in a so-called *doubly*

stochastic Poisson process (Saleh, 1978), where one stochastic process is used to generate the rate of a second one. Such a process was postulated to characterize—successfully—a number of properties of retinal ganglion cell spike trains at low light levels (Saleh and Teich, 1985). In this limit, the distribution of photons absorbed at the retina is expected to be Poisson. If each photon results in a slowly decaying input current to a ganglion cell that generates on average two spikes per incoming photon, the interspike interval distribution of the model will have a C_V greater than 1. The cause of this additional variability lies in the random number of spikes generated for each incoming Poisson pulse (Gabbiani and Koch, 1998).

Special care must be taken when analyzing the variability of bursting cells (see the following chapter). If a bursty cell switches between bursting and nonbursting, the variability of its interspike intervals can be larger than that of a Poisson process, that is, $C_V > 1$ (Wilbur and Rinzel, 1983). Numerical techniques have been developed to account for the highly correlated adjacent interspike intervals that occur during bursting (a measure termed C_{V2}; Holt et al., 1996).

15.2.3 Spike Count and Fano Factor

So far, we have restricted ourselves to a consideration of the temporal jitter. However, neurons show considerable variation in the number of spikes triggered in response to a particular stimulus. This can be quantified by the ratio of the variance of the number of spikes generated within some observational window T to the mean number of spikes within the same time period, the so-called *index of dispersion* or *Fano factor* (Fano, 1947),

$$F(T) = \frac{\mathrm{Var}[N(T)]}{\langle N(T) \rangle}. \tag{15.18}$$

Counting Poisson distributed spikes of mean rate μ over an observational interval of duration T, leads to a mean number of spikes $T\mu$ with variance $T\mu$. In other words, for an ideal Poisson process, no matter for what duration it is observed, $F(T) = 1$.

Experimentally, $F(T)$ should be estimated by computing the average number of spikes and their variance for a fixed counting time T using many repetitions of the same stimulus. The counting time should now be systematically varied over the range of interest.[3] The Fano factor is usally plotted in log-log coordinates, and the slope of the best fit through these points is reported. For a true Poisson process, the slope is 1. Slopes bigger than 1 imply that the variance in the number of events grows faster than the mean, indicating long-term correlations in the data.[4]

As illustrated in Fig. 15.6, the $F(T)$ factor in different neural systems is frequently close to unity for observational times on the order of 100 msec, compatible with the Poisson hypothesis (modified by a refractory period that lowers $F(T)$ to a value slightly less than unity; Teich, 1992). Yet for large windows, say in the second to minute domain, long-term trends in the data are very apparent (revealed by the very large $F(T)$ values). These are most likely due to state changes in the underlying neural networks. Obviously, modeling data over these time spans forces abandonment of the Poisson hypothesis. In some sensory systems $F(T)$ can be considerably less than 1 (van Steveninck et al., 1997; Berry, Warland, and Meister, 1997).

---

3. A frequently used approximation is to estimate $(\langle N \rangle, \mathrm{Var}[N])$ for a fixed trial, say of 1 sec duration. This procedure is repeated under circumstances (that is, by varying the stimulus intensity) that give rise to different values of $\langle N \rangle$.

4. Indeed, the Fano factor can be related to the autocorrelation function of the underlying point process (Gabbiani and Koch, 1998).

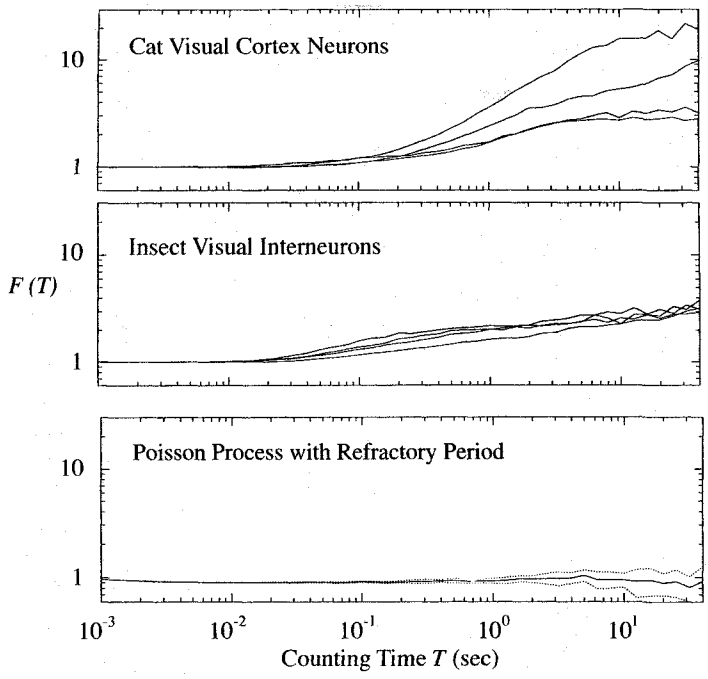

Fig. 15.6 Variability in Spike Count Fano Factor (Eq. 15.18), that is, the variance of the number of spikes normalized by their mean, within an observational counting window of duration T in different spiking systems. The top panel shows $F(T)$ for the spontaneous activity of four cells taken from the visual cortex of the anesthetized cat (Teich et al., 1997). For $T < 0.1$ sec, the variability is close to unity, as expected from a Poisson process. However, for larger observational windows, $F(T)$ strongly increases, indicative of long-term correlations in the firing behavior, possibly due to slow state changes in the cat. The qualitatively same behavior for spontaneous activity can be observed in the middle panel, plotting $F(T)$ for four visual interneurons in the cricket (Turcott, Barker, and Teich, 1995), although $F(T)$ is not as large as in the cortex. The lower plot illustrates $F(T)$ (along with its standard deviation) associated with 10 simulated runs of a Poisson process with a refractory period. Since a refractory period imposes some degree of order, $F(T)$ is less than that of a pure Poisson process but still close to unity. Reprinted by permission from Teich, Turcott, and Siegel (1996).

In general, the jitter in the timing of events need not be related to the jitter in the number of events. Under conditions when the spiking can be described as a *renewal process*, that is, if the interspike intervals are independently and identically distributed, the distribution of spike counts for long observation times will be approximately Gaussian distributed. Since the same is true for the interspike interval distribution (e.g., Fig. 15.4C), these two measures are related via

$$F = C_V{}^2 \tag{15.19}$$

in the limit as the observational period $T \to \infty$ (Cox, 1962). This is a property of spike trains that is not widely appreciated.

Many studies have measured interspike intervals as well as spike count variability, although usually not simultaneously, of spontaneous or stimulus-induced activity. One of the aims is to infer something about the dynamics of the spiking threshold or about the different states the neuron can be in (Werner and Mountcastle, 1963; Smith and Smith, 1965; Calvin and Stevens, 1967, 1968; Noda and Adey, 1970; Burns and Webb, 1976;

Vogels, Spileers, and Orban, 1989; Snowden, Treue, and Andersen, 1992; Softky and Koch, 1993; Usher et al., 1994; Turcott, Barker, and Teich, 1995; Teich, Turcott, and Siegel, 1996; Teich et al., 1997). It was only recently that attempts have been made to reconcile the observed high variability of neurons with the known biophysical properties of single cells and network properties. In order to discuss some of these, let us now throw inhibition into the brew.

15.2.4 Random Walk Model of Stochastic Activity

We do this in the form of adding an inhibitory synaptic process of rate μ_i and weight $a_i > 0$. Now the random process $V(t)$ undergoes random "up" jumps (of amplitude a_e) and "down" jumps (of amplitude a_i; Fig. 15.7). In the absence of a threshold, the potential can be modeled by

$$V(t) = a_e N_e(t) - a_i N_i(t)\,, \tag{15.20}$$

with $V(0) = 0$ and $V < V_{\text{th}}$. The expected value of this process follows from the fact that Eq. 15.20 is linear, as

$$\langle V(t)\rangle = a_e\langle N_e(t)\rangle - a_i\langle N_i(t)\rangle \tag{15.21}$$

$$= a_e\mu_e t - a_i\mu_i t = \mu t\,, \tag{15.22}$$

where $\mu = a_e\mu_e - a_i\mu_i$ is termed *drift*. The variance of the voltage over time is

$$\text{Var}[V(t)] = a_e{}^2\text{Var}[N_e(t)] + a_i{}^2\text{Var}[N_i(t)] \tag{15.23}$$

$$= a_e{}^2\mu_e t + a_i{}^2\mu_i t = \sigma^2 t\,, \tag{15.24}$$

where $\sigma^2 = a_e^2\mu_e + a_i^2\mu_i$ is called the *variance parameter*. The drift corresponds to the net input current into the unit. As long as it is different from zero, the average membrane potential as well as the jitter will diverge (in the absence of either a leak or a threshold). Note that the standard deviation around $\langle V\rangle$ increases as the square root of time, reminiscent of the jitter in the motion of a particle diffusing in one or more dimensions (Sec. 11.1). This is not surprising, since both represent instances of *random walks*. (For an introduction into the theory of the random walk, see Feller, 1966, or Berg, 1983.)

The probability distribution of $V(t)$ in the absence of any threshold and membrane leak can be computed analytically. We spare the reader its derivation, referring him or her instead to Eq. 9.42 in the monograph by Tuckwell (1988b). Figure 15.7A illustrates one particular realization of the random process $V(t)$, together with $\langle V(t)\rangle$ and its associated jitter.

Will the membrane potential ever reach threshold V_{th} and generate a pulse? And how long is this event expected to take? This question, known as the "time of first passage to threshold" problem, has a nontrivial but well characterized probability density function $f_{\text{th}}(t)$ associated with it (see Eq. 9.54 in Tuckwell, 1988b and Fig. 15.7B). If T_{th} is the random time taken for V to go from its initial state at $V = 0$ to $V = V_{\text{th}}$, one can estimate that

$$\Pr\{T_{\text{th}} < \infty\} = \int_0^\infty f_{\text{th}}(t)dt \tag{15.25}$$

or

$$\Pr\{T_{\text{th}} < \infty\} = \begin{cases} 1 & \text{if } \mu \geq 0 \\ (a_e\mu_e/a_i\mu_i)^{V_{\text{th}}} & \text{if } \mu < 0. \end{cases} \tag{15.26}$$

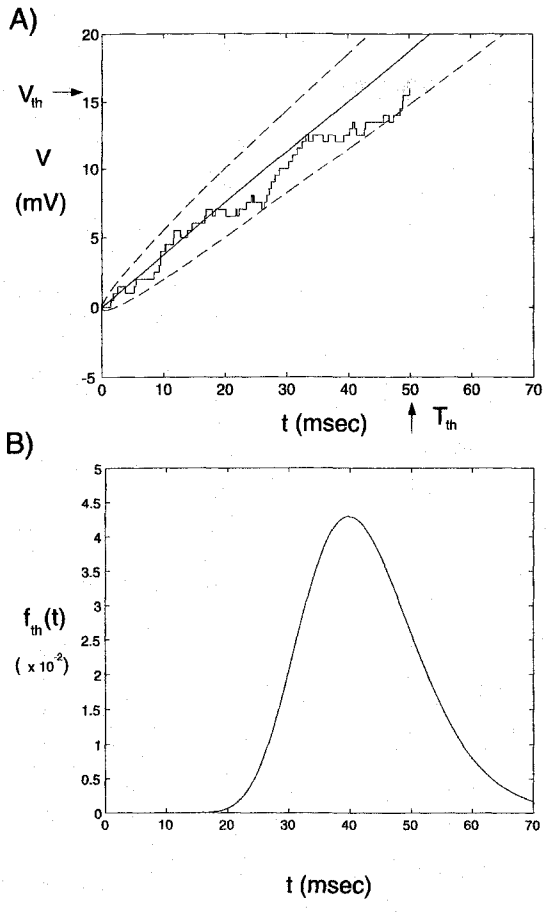

Fig. 15.7 Random Walk of the Membrane Potential Illustration of the random walk model of excitatory and inhibitory synaptic input into a nonleaky integrate-and-fire unit as pioneered in this form by Stein (1965). The cell receives Poisson distributed excitatory input (with rate $\mu_e = 1000$ Hz), each increasing the voltage by 0.5 mV, and Poisson distributed inhibitory input (at a rate of 250 Hz), each input decreasing the potential by 0.5 mV. Threshold is reached at 16 mV. **(A)** One instantiation of such a random walk, together with the expected mean potential and its standard deviation. The unit generates a spike at around $T_{\text{th}} = 50$ msec. **(B)** Probability density $f_{\text{th}}(t)$ for the first passage to threshold, that is, for the time it takes before the voltage threshold is reached for the first time.

If the drift is positive, the unit will eventually spike with probability 1. If the net input is negative, then one must wait for a fluctuation in the input to elevate V to threshold. This is less and less likely as the effective inhibition exceeds excitation with a finite chance that threshold is never reached.

In the former case, that is, for $a_e\mu_e > a_i\mu_i$, we can easily compute the first and second moments associated with T_{th}. Specifically, the mean time to fire is

$$\langle T_{\text{th}} \rangle = \frac{V_{\text{th}}}{\mu} \tag{15.27}$$

and the variance of this mean is

$$\text{Var}[T_{\text{th}}] = V_{\text{th}} \frac{a_e\mu_e + a_i\mu_i}{\mu^3}. \tag{15.28}$$

Because we assume that the unit had started out at $V = 0$ (implying that it had just spiked and was reset), T_{th} corresponds to the average interval between adjacent spikes. While we are unable to predict the exact trajectory of the membrane potential, we can perfectly well predict certain time-averaged aspects of spike trains.

The normalized "width" of the ISI, expressed by the coefficient of variation, is

$$C_V = \frac{(\text{Var}[T_{\text{th}}])^{1/2}}{\langle T_{\text{th}} \rangle} = \left(\frac{1}{V_{\text{th}}} \frac{a_e \mu_e + a_i \mu_i}{a_e \mu_e - a_i \mu_i} \right)^{1/2} . \tag{15.29}$$

Setting $\mu_i = 0$ in these expressions gives us back our earlier equations. Adding in inhibition leads to the expected result that the mean membrane potential decreases and that $\langle T_{\text{th}} \rangle$ increases. A bit less expected is that the variance of $\langle V \rangle$ as well as the jitter associated with $\langle T_{\text{th}} \rangle$ both increase. Intuitively, this can be explained by noting that we are adding a new source of unpredictability, even if it is inhibitory. Indeed, by adding enough inhibition one can always achieve a situation in which the drift is close to zero but the jitter becomes very large. This is termed *balanced inhibition* or *balanced excitation and inhibition* and was first investigated by Gerstein and Mandelbrot, 1964 (for more recent accounts, see Shadlen and Newsome, 1994; Tsodyks and Sejnowski, 1995 and, in particular, van Vreeswijk and Sompolinsky, 1996). Since the amount of inhibition increases in parallel with the amount of excitation, threshold is not reached by integrating a large number of small inputs over time (as with $\mu > 0$), but by a large enough "spontaneous" positive fluctuation in excitation, complemented by a large enough downward fluctuation in inhibition. This is of course much less likely to occur than if the drift is large (and positive).

A straightforward generalization of these results involves more than two synaptic processes. Conceptually, one process that is Poisson distributed with rate μ and amplitude a can always be replaced by n processes, all independent of each other, firing at rate μ/n and amplitude a, or by n independent processes of rate μ but of amplitude a/n. Indeed, all we need to assume is that the synaptic inputs impinging onto the cell derive from the superposition of arbitrary point processes that are independent of each other. If these processes are stationary (see above), the superposition of such processes will converge to a stationary Poisson process (Cox and Isham, 1980).

Finally, we do not want to close this section without briefly mentioning *Wiener processes* or *Brownian motion*. What makes the mathematical study of the random walk models discussed so far tortuous is that each sample path is discontinuous, since upon arrival of a synaptic input, $V(t)$ changes abruptly by $\pm a$. The associated differential-difference equations are less well understood than standard differential equations. Introduced into the neurobiological community by Gerstein and Mandelbrot (1964), Wiener processes are thoroughly studied and many of the relevant mathematical problems have been solved. A Wiener process can be obtained as a limiting case from our standard random walk model by letting the amplitude a of each synapse become smaller and smaller, while the rate at which the input arrives becomes faster and faster. In the appropriate limit one obtains a continuous sample path, albeit with derivatives that can diverge (indeed the "derivative" of the path is *white noise*). The crucial difference as compared to the discrete Poisson process is that for any two times t_1 and t_2, $V(t_2) - V(t_1)$ is a continuous Gaussian random variable with zero mean and variance $(t_2 - t_1)$ (whereas for the random walk models, $V(t_2) - V(t_1)$ takes on discrete values). Because the basic intuition concerning the behavior of a simple nonleaky integrate-and-fire model can be obtained with the random walk model discussed above, complemented by computer simulations

that are to follow, we shall not treat Wiener processes here, referring the reader instead to Tuckwell (1988b).

15.2.5 Random Walk in the Presence of a Leak

So far, we neglected the presence of the membrane leak resistance R, which will induce an exponential voltage decay between synaptic inputs, leading to "forgetting" inputs that arrived in the past compared to more recent arrivals. It was Stein (1965) who first incorporated a decay term into the standard random walk model. Heuristically, we need to replace Eq. 15.19 by

$$C\frac{dV}{dt} = -\frac{V}{R} + a_e\frac{dN_e}{dt} - a_i\frac{dN_i}{dt}. \tag{15.30}$$

Because the trajectories of both N_e and N_i are discontinuous, jumping by ± 1 each time a synaptic input arrives, dN/dt can be thought of as a series of delta functions, increasing V abruptly by a_e (or decreasing by a_i). In the absence of any threshold, the mean membrane potential is

$$\langle V(t)\rangle = R(a_e\mu_e - a_i\mu_i) = R\mu \tag{15.31}$$

where the drift $\mu = a_e\mu_e - a_i\mu_i$ has the dimension of a current.[5] Equation 15.31 was derived under the assumption that the initial value of the membrane potential has decayed away as $e^{-t/\tau}$, with $\tau = RC$.

Different from the nonleaky case, where the membrane potential diverges (as $\langle V(t)\rangle = \mu t/C$ in physical units; see Eq. 15.21), the membrane leak stabilizes the membrane potential at a level proportional to the drift, that is, the mean input current. The variance will also remain finite

$$\mathrm{Var}[V(t)] = \frac{1}{2}\frac{R}{C}(a_e{}^2\mu_e + a_i{}^2\mu_i) = \frac{1}{2}\frac{R}{C}\sigma^2. \tag{15.32}$$

It is straightforward to generalize this to the case of n inputs.

What about the mean time to spike? Unfortunately, even after several decades of effort, no general expressions for the probability density of T_{th} and related quantities, such as the ISI distribution, are available and we have to resort to numerical solutions. Qualitatively, the leak term has little effect on the ISI for high rates, because there is not sufficient time for any significant fraction of the charge to leak away before V_{th} is reached. In other words, we can neglect the effect of a leak if the interspike interval is much less than τ.

At low firing rates, the membrane potential "forgets" when the last firing occurred, so that the subsequent firing time is virtually independent of the previous time. In this mode, the leaky integrator operates as a "coincidence" detection device for occasional bursts of EPSPs. More interspike intervals will occur at large values of t than expected from the model without a leak and the associated C_V value is larger than for the nonleaky integrator.

A number of attempts have been made to include stochastic synaptic activity into distributed cable models, including solving the cable equation in the presence of white noise current (Tuckwell and Wan, 1980; see also Chap. 9 in Tuckwell, 1988b). Since the complexity of these models usually precludes the development of useful intuition concerning the computational properties of nerve cells, we will not discuss them any further and refer the reader to Tuckwell (1988b,c).

5. In the previous pages we assumed—implicitely, for the most part—that each synaptic input increases the membrane potential by a_e/C although we did not explicitly write out the dependency on C.

15.3 What Do Cortical Cells Do?

So, how random are cortical cells? And is their observed degree of variability compatible with their known biophysics?

Before we discuss this, a word of caution. The majority of experimental studies assume that the statistics of spikes do not vary significantly during the period of observation. Since this degree of stationarity is very difficult to verify empirically, a more reasonable concept is that of a weakly stationary process, for which only the mean and the covariance need to be invariant under time translation. For a spike train generated in response to a physiological stimulus (such as a flashed bar of light) nonstationarity is practically guaranteed since both single-cell and network effects conspire to lead to firing frequency adaptation. This is reflected in the poststimulus time histogram, which usually is not flat (e.g., Fig. 15.1). Several techniques exist to deal with such nonstationary data (for instance, by only using the adapted part of the spike train or by normalizing for the local rate $\mu(t)$; Perkel, Gerstein, and Moore, 1967; Softky and Koch, 1993).

Investigating the response of cat motoneurons in the spinal cord to intracellular current injections, Calvin and Stevens (1967, 1968) concluded that in two out of five cells they considered in great detail, the low degree of observed jitter in spike timing ($C_V \approx 0.05$) could be explained on the basis of noisy synaptic input charging up the somatic potential until it reaches V_{th} and triggers a spike (Fig. 15.8A). This is expected if the cell behaved like an ideal integrate-and-fire unit under the random walk assumptions (Eq. 15.21).

15.3.1 Cortical Cells Fire Randomly

What about cells in the cerebral cortex? How randomly do they fire? And what does their surprisingly high degree of randomness imply about the neural code used for information transmission? Anecdotal evidence (Fig. 15.8B) illustrates that under certain conditions, the somatic membrane potential of cortical neurons does behave as expected from the random walk model discussed above, integrating a large number of small inputs until threshold is reached. But is this really compatible with their variability? Although the firing variability of thalamic and cortical cells has been studied experimentally for quite some time, this was caried out predominantly during spontaneous firing, when rates are very low (Poggio and Viernstein, 1964; Noda and Adey, 1970; Burns and Webb, 1976; Teich, Turcott, and Siegel, 1996). Softky and Koch (1992, 1993) measured the firing variability of cells from cortical areas V1 and MT in the awake monkey responding to moving bars and random dots with maintained firing rates of up to 200 Hz. Applying appropriate normalization procedures and excluding bursting cells, Softky and Koch found that C_V was close to unity—as expected from a Poisson process (Fig. 15.9).

This poses somewhat of a paradox. At high enough firing rates, when the decay of the membrane potential can be neglected, C_V is inversely proportional to the square root of n_{th}, the number of excitatory inputs necessary to trigger threshold (Eq. 15.16). If n_{th} is large, as commonly held (that is, 20, 50, or 100),[6] the cell should fire in a very regular manner, which cortical cells patently do not do. On the basis of detailed compartmental simulations of a cortical cell with passive dendrites, Softky and Koch (1993) showed that

6. Based on evidence from spike-triggered averaging, in which spikes recorded in one neuron are correlated with monosynaptic EPSPs recorded in another pyramidal cell; the amplitudes usually fall below 0.5 mV (Mason, Nicoll, and Stratford, 1991; for a review see Fetz, Toyama, and Smith, 1991). This implies that on the order of 100 simultaneous excitatory inputs are required to bring a cortical cell above threshold.

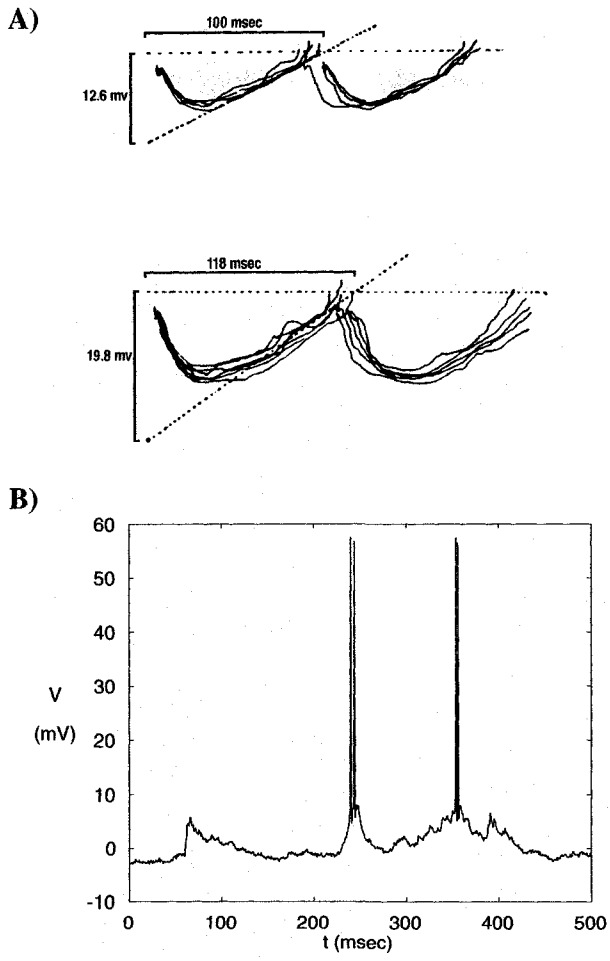

Fig. 15.8 Does the Membrane Potential Drift up to V_{th}? Intracellular membrane potential in two different cell types. **(A)** Somatic potential in a motoneuron in the spinal cord of an anesthetized cat in response to a constant intracellular current injection (Calvin and Stevens, 1968). Portions of the membrane potential between adjacent spikes are superimposed, matched against a theoretical model in which the depolarization to threshold is expected to be linear in time (Eq. 15.22) and evaluated against a fixed V_{th} (dotted horizontal line). This model explains the jitter in spike timing in two out of five motoneurons investigated entirely on the basis of synaptic input noise. Reprinted in modified form by permission from Calvin and Stevens (1968). **(B)** Intracellular recording from a complex cell in cat visual cortex (Ahmed et al., 1993), responding to a bar moving in the preferred direction. The depolarizing event around 80 msec was not quite sufficient to generate a spike. This cell does appear to integrate over many tens of milliseconds, as witnessed by the slow rise and fall of the membrane potential. It remains a matter of intense debate whether spiking in cortical cells can be explained by treating the cell as integrating over a large number of small excitatory and inhibitory inputs or whether cortical cells detect coincidences in synaptic input at a millisecond or finer time scale. Unpublished data from B. Ahmed and K. Martin, printed with permission.

neither (1) distributing synaptic inputs throughout the cell, (2) including Hodgkin-Huxley-like currents at the soma, (3) incorporating a "reasonable" amount of synaptic inhibition, nor (4) using weakly cross-correlated synaptic inputs changed this basic conclusion appreciably.

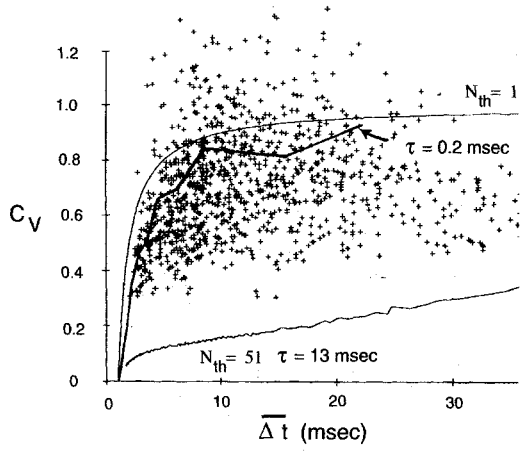

Fig. 15.9 FIRING VARIABILITY OF CELLS IN MONKEY CORTEX Comparison of the variability of spike timing, quantified using the coefficient of variation C_V, as a function of the mean interspike interval for cortical cells and modeled data. The scattered crosses are from V1 and MT cells recorded in the behaving monkey and are normalized for their mean firing rates. Their C_V is high, close to unity. Superimposed are the C_V curves computed for a random walk leaky integrate-and-fire model using conventional assumptions (lower trace; $n_{th} = 51$, $\tau = 13$ msec, and $t_{ref} = 1$ msec) and less conventional ones (middle bold trace; $n_{th} = 51$ and $\tau = 0.2$ msec). The thin, top curve corresponds to the limiting case of a pure Poisson spike train ($n_{th} = 1$) in combination with $t_{ref} = 1$ msec. The effect of this absolute refractory period is to render the spike timing very regular at very high firing rates. Reprinted in modified form by permission from Softky and Koch (1993)

Cortical cells cannot integrate over a large number of small synaptic inputs and still fire as irregularly as they do. Instead, either the time constant of the cell has to be very small, in the 1 msec range (in which case synaptic input that arrived more than 2 or 3 msec ago has been forgotten), or n_{th} must be very small, in the neighborhood of 2–5 (Fig. 15.9).

Measuring variability in the spike count confirmed this high degree of randomness. Log-log plots of the mean versus the variance in the number of spikes in the cortex of the monkey consistently give rise to slopes of around 5/4, implying large values for $F(T)$ (Tolhurst, Movshon, and Dean, 1983; Zohary, Hillman, and Hochstein, 1990; Snowden, Treue, and Andersen, 1992; Softky and Koch, 1993; Teich, Turcott, and Siegel, 1996). As before, the standard integrator model of pyramidal cells should lead to much smaller values of the Fano factor $F(T)$.

15.3.2 Pyramidal Cells: Integrator or Coincidence Detector

Softky and Koch (1992, 1993) argue for a *coincidence detection* model in which distal dendrites generate fast sodium action potentials which are triggered when two or more excitatory synaptic inputs arrive within a millisecond of each other. A handful of these active synaptic events, if coincident at the soma, will trigger a spike. (This effectively reduces n_{th} to the required small values.) Indeed, Softky (1994, 1995) claims that the experimental evidence for active dendritic conductances is compatible with submillisecond coincidence detection occurring in the dendrites of pyramidal cells (see Sec. 19.3.3).

This has rekindled a debate over the extent to which pyramidal cells either integrate over many small inputs on a time scale of tens of milliseconds or detect coincidences at

the millisecond or faster time scale (Abeles, 1982b; Shadlen and Newsome, 1994; König, Engel, and Singer, 1996). In the former case, the code would be the traditional noisy rate code that is very robust to changes in the underlying hardware. If neurons do use precise spike times—placing great demands on the spatio-temporal precision with which neurons need to be wired up—the resultant spike interval code can be one or two orders of magnitude more efficient than the rate code (Stein, 1967a,b; Rieke et al., 1996).

As illustrated in Fig. 15.10A, the Geiger counter model leads to very regular spiking, since the cell integrates over a large number of inputs (here $n_{\text{th}} = 300$). High irregularity of the spike discharge can be achieved in several ways. If the neuron has a very short time constant, it will only fire if a sufficient number of spikes arrive within a very small time. Such a coincidence detector model is illustrated in Fig. 15.10B and is simulated by considering V to be the sum of all EPSPs arriving within the last millisecond. If at least 35 EPSPs are coincident within this time, an output spike is generated. This model is, of course, sensitive to disturbances in the exact timing of the synaptic input. It is precisely this sensitivity that can be used to convey information.

Shadlen and Newsome (1994), Tsodyks and Sejnowski (1995), and van Vreeswijk and Sompolinsky (1996) seek an explanation of the high variability in a *balanced inhibition* random walk, in which the drift is zero (as in Gerstein and Mandelbrot, 1964), that is, the average net current is zero, excitation balancing inhibition. The unit spikes whenever a fluctuation leads to a momentary drop in synaptic inhibition in combination with a simultaneous excess of excitation. (This is achieved in Fig. 15.10C by having the 150 inhibitory cells fire at the same rate as the 300 excitatory cells, but with twice their postsynaptic weight.)

It can be shown analytically (van Vreeswijk and Sompolinsky, 1996) that large networks of simple neurons, randomly and sparsely interconnected with many relatively powerful excitatory and inhibitory synapses whose activity is approximately "balanced," display highly irregular patterns of spiking activity characteristic of *deterministic chaos*. Such networks can respond very rapidly to external input, much faster than the time constant of the individual neurons. van Vreeswijk and Sompolinsky (1996) argue that irregular spiking is a robust emergent network property not depending on intricate cellular properties. Yet this ability to respond rapidly comes at a price of continual activity, requiring a constant expenditure of metabolic energy. Experimentally, it remains an open question to what extent individual cells receive balaced input, that is to what extent sustained changes in excitatory input are opposed by equally powerful sustained changes in inhibition.

A related solution to the dilemma of obtaining high variability while retaining the integrating aspect of cortical cells is correlated synaptic inputs. If excitatory synaptic inputs have a tendency to arrive simultaneously, less temporal dispersion will occur and inputs will be more effective. Voltage-dependent sodium conductances in the dendritic tree will be particularly sensitive to such simultaneous inputs, effectively lowering the number of inputs needed to reach threshold.

Including more complex spike generation dynamics, such as bursting (Wilbur and Rinzel, 1983; but see Holt et al., 1996), or incorporating short-term adaptation into the synapses (Abbott et al., 1997; Sec. 13.5.4) will increase C_V and $F(T)$. The somewhat arbitrary choice of resetting the membrane potential following spike generation to the unit's resting potential offers yet another way to increase variability. Intracellular data from cortical cells frequently reveal the lack of any hyperpolarization following an action potential. Bell et al., (1995) and Troyer and Miller (1997) argue that the membrane potential should be reset to a much more positive value, thereby lowering the effective n_{th}.

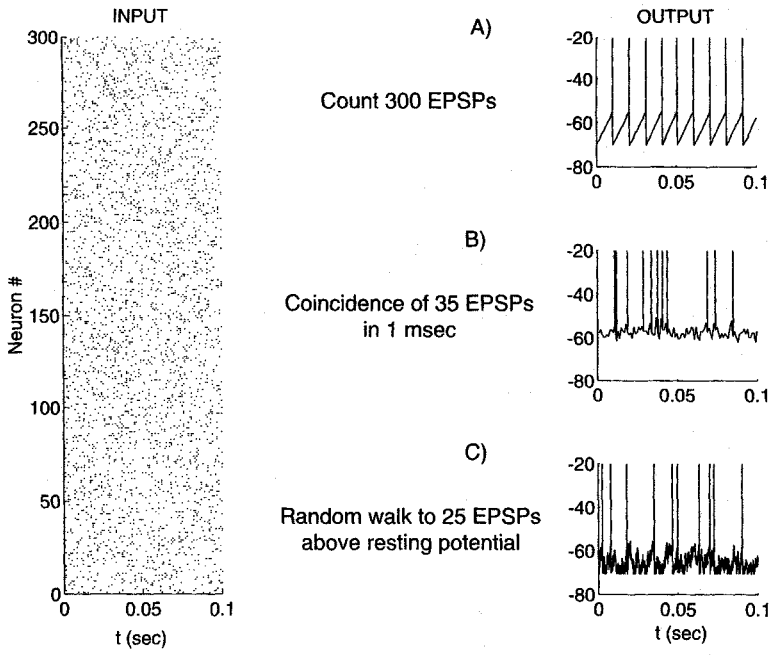

Fig. 15.10 THREE MODELS OF SYNAPTIC INTEGRATION The input to the simulated neuron is shown in the left panel: 300 excitatory Poisson distributed synaptic inputs, firing at a mean rate of $\mu_e = 100$ Hz. The output units on the right also fire at this average rate. **(A)** Ideal integrate-and-fire model. Each synaptic input increases V by 0.05 mV, corresponding to $n_{\text{th}} = 300$. As expected, the output pulses have a clocklike regularity. **(B)** In this cartoon of a coincidence detector model, only inputs within the previous millisecond contribute toward V (corresponding to an effective submillisecond time constant). If $n_{\text{th}} = 35$ EPSPs arrive "simultaneously" (here, within 1 msec), the unit spikes. Notice the elevated mean membrane potential. In this model, the timing of spikes can code information. **(C)** Standard random walk model with a balance of excitation and inhibition. In addition to the 300 excitatory inputs, 150 inhibitory inputs have been added, firing at the same rate; $a_e = 0.6$ mV (corresponding to an effective $n_{\text{th}} = 25$) and $a_i = 1.2$ mV. This model achieves a high variability but at a cost of substantial inhibition. Since no information is encoded in the time of arrival of spikes, it is very robust. Adding a leak term to the first and third models does not affect these conclusions substantially. Reprinted by permission from Shadlen and Newsome (1994)

What is clear is that the simple Geiger counter model of synaptic integration needs to be revised. A plethora of mechanisms—such as synaptic inhibition, short-term synaptic depression, correlated synaptic input, a depolarizing reset, active dendritic processing on a fast time scale—will interact synergistically to achieve the observed random behavior of cortical cells.

Lest the reader forget the cautionary note posted earlier, the preceding paragraphs apply specifically to cortical cells. Given the great diversity apparent in the nervous system, the question of the variability of neuronal firing and its implication for the code must be investigated anew in each specific cell type. In cells where synaptic input but modulates the strongly nonlinear dynamics of firing, as in oscillatory or bursting cells (Jaeger, DeSchutter, and Bower, 1997; Marder and Calabrese, 1996), the source of variability could be quite distinct from those discussed here.

15.3.3 Temporal Precision of Cortical Cells

Yet under some conditions, cortical spike trains can look remarkably consistent from trial to trial. This is exemplified in a quite dramatic manner by Fig. 15.11, from an experiment carried out in a monkey that had to respond to various patterns of random dot motion (Newsome, Britten, and Movshon, 1989). If one averages—as is frequently done in practice—over many such presentations of different clouds of randomly moving dots, the spiking activity of the cell looks uneventful (beyond the initial transient; left column). Yet if one pulls out all of the responses to exactly the same random dot movie, a highly repeatable pattern of spiking becomes visible. Such reliable responses could be observed in the majority of MT cells examined (Bair and Koch, 1996). These stimulus-induced temporal modulations disappear for coherent motion, that is, when the entire cloud of dots moves as one across the receptive field, explaining why they are not visible in Fig. 15.1 (Bair, 1995).

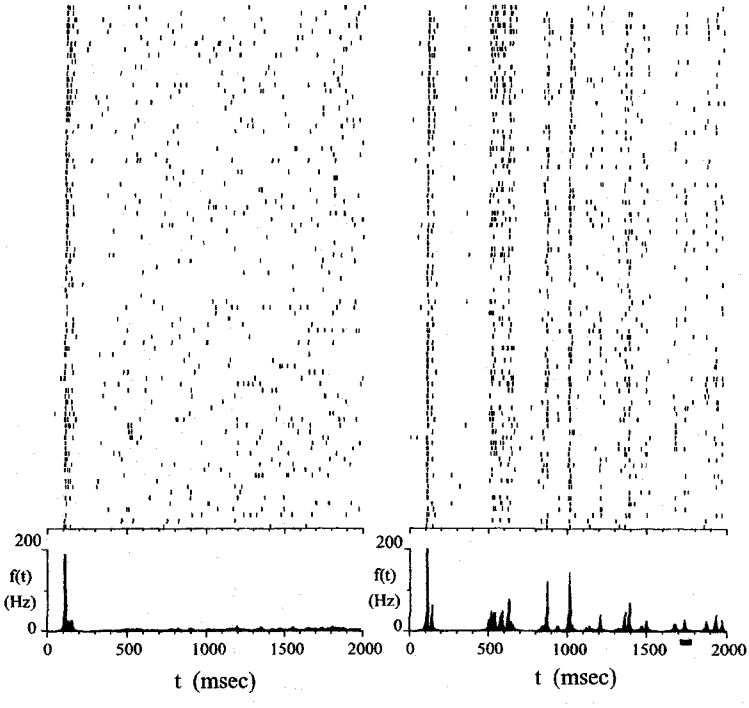

Fig. 15.11 Cortical Cells Can Fire in a Very Precise Manner Responses of an MT cell in a behaving monkey to patterns of randomly and independently moving dots. The left column shows the cortical response to different random dot patterns. Averaged over 90 trials, the cell's response is well described by a random point process with $\mu = 3.4$ Hz (excluding the initial "flash" response; see the bottom panel). When only trials over the 2-hour-long experiment that were stimulated by the identical random dot movie are considered (right column), strikingly repeating patterns can be observed. (Viewing this figure obliquely best reveals the precision of spiking.) Notice the sharp peak following the 1-sec mark or that nearly all spikes in the final 400 msec cluster into six vertical streaks. Despite this precision, observed in the majority of MT cells, spike count variability $F(T)$ is still very high. The poststimulus time histogram, using an adaptive square window, is shown at the bottom. Reprinted by permission from Bair and Koch (1996).

When contemplating Fig. 15.11, it should be kept in mind that at the beginning of the experiment, the animal is thirsty and eager to perform, while at the end it is satiated and not very motivated. Furthermore, the animal continuously makes small eye movements, termed microsaccades. Yet despite this, a cell removed at least six synapses from the visual input fires in a very repeatable pattern throughout this time.

Bair and Koch (1996) quantify the degree of precision by computing the temporal jitter, that is, the standard deviation in time of the onset of periods of elevated firing (such as the "event" indicated by a black bar near 1740 msec in Fig. 15.11; see also Sestokas and Lehmkuhle, 1986). For this event, the jitter is 3.3 msec. For 80% of all cells, the most precise response has a jitter of less than 10 msec, while in some cases it is as low as 2–4 msec.

Although somewhat counterintuitive, even these spike trains can be generated by a Poisson process, but in this case with a time-varying rate $\mu(t)$ (called *inhomogeneous* Poisson process). As in a homogeneous Poisson process, the number of spikes in any one time interval is independent of the number of spikes in any other nonoverlapping interval. The time intervals between adjacent spikes also remain independent of each other but are not identically distributed anymore (Tuckwell, 1988b). In the case of the data shown in Fig. 15.11, the Fano factor $F(T)$ is close to unity when evaluated for the duration of the stimulus (Britten et al., 1993).

We conclude that individual cortical cells are able to reliably follow the time course of events in the external world with a resolution in the 5–10 msec range (see also Mainen and Sejnowski, 1995).

Let us hasten to add that much evidence has accumulated (as cited in Sec. 14.1) indicating that the precision of spike generation in one cortical cell with respect to another cell's firing can be even higher (e.g., Lestienne and Strehler, 1987). Best known is the demonstration of repeating patterns among simultaneously recorded cells by Abeles et al., (1993). Pairs of cells may fire action potentials at predictable intervals that can be as long as 200 msec, two orders of magnitude longer than the delay due to a direct synaptic connection, with a precision of about 1 msec. This is the key observation at the heart of Abeles's *synfire chain* model of cortical processing (Abeles, 1990).

Any rash judgment on whether or not the detailed firing pattern is noise or signal should be tempered by Barlow's (1972) statement about the firing of individual nerve cells that "their apparently erratic behavior was caused by our ignorance, not the neuron's incompetence."

15.4 Recapitulation

In this chapter we tried to address and quantify the stochastic, seemingly random nature of neuronal firing. The degree of randomness speaks to the nature of the neural code used to transmit information between cells. Very regularly firing cells are obviously not very good at encoding information in their timing patterns; yet this will not prevent information from being encoded in their mean firing rates, albeit at a lower rate (in terms of bits per spike) but in a robust manner.

The spiking behavior of cells has traditionally been described as a random point process, in particular as a renewal process with independent and identically distributed interspike intervals. Cortical cells firing at high rates are at least as variable as expected from a simple Poisson process. Variability is usually quantified using two measures: C_V to assess the interspike interval variability and $F(T)$ for spike count variability, with both taking on

unity for a Poisson process. If spike trains are generated by a renewal process, $F = C_V^2$ in the limit of large observational intervals.

The power spectrum of cortical spike trains is flat with a dip around the origin, as expected from a Poisson process modified by a refractory period. (This refractory period only comes into play at very high firing rates, serving to regularize them.) The rate of the spiking process is usually not constant in time, but is up or down regulated at the 5–10 msec level. The principal deviation from Poisson statistics is the fact that adjacent interspike intervals are not independent of each other (even when neglecting bursting cells), that is, spike trains cannot really be described by a renewal process.

As always in science, this conclusion gives birth to intertwining considerations. What type of models of synaptic integration give rise to the high degree of randomness apparent in neuronal firing and how do these constrain the nature of the neuronal code? The standard Geiger counter model predicts that when an integrate-and-fire unit needs to integrate over a large number of small synaptic inputs, it should fire very regularly. Since this is patently not true in the cortex, it needs to be abandoned. Out of the many alternatives proposed, two divergent views crystallize. One school retains the idea that neurons integrate over large number of excitatory inputs with little regard for their exact timing by invoking a large degree of inhibitory inputs (following the random walk model advocated by Gerstein and Mandelbrot, 1964), a depolarizing reset, or correlated synaptic input. The other school sees cortical cells as coincidence detectors, firing if small numbers of excitatory events arrive simultaneously at the millisecond (or even submillisecond) scale (via powerful and fast dendritic nonlinearities). Under these circumstances, detailed timing information can be used to transmit information in a manner much more efficient, yet also more demanding, than in a mean rate code. Only additional experimental evidence can resolve this issue.

Of course, at small enough time scales or for a handful of spikes, the debate loses its significance, since it becomes meaningless to define a rate for a 20 msec long segment of a spike train with just two action potentials.

What this dispute shows is that integrate-and-fire units serve as gold standard against which models of variability are evaluated. Given their relative simplicity—compared against the much more complex conductance-based models of firing—this is quite remarkable.

The highly variable character of cortical firing allows neurons to potentially pack one or more bits of information per action potential into spike trains (as done in sensory neurons closer to the periphery). Information theory as applied to a band-limited communication channel has taught us that the optimal code—optimal in terms of using the entire bandwidth available—looks completely random, since every redundancy has been removed to increase the efficiency. One could infer from this that neurons make optimal use of the limited bandwidth of axons using a sophisticated multiplexed interspike interval code from which all redundancies have been removed, and that neurons, properly decoded, maximize the existing channel bandwidth. To what extent they actually do for physiologically relevant stimuli remains an open issue.